

## GROUND TESTS OF HIGH-VOLTAGE SOLAR ARRAYS IMMERSSED IN A LOW DENSITY PLASMA

Boris Vayner \*

Ohio Aerospace Institute, Cleveland, OH

Joel Galofaro<sup>\*</sup>, and Dale Ferguson<sup>§</sup>

NASA Glenn Research Center, Cleveland, OH

### ABSTRACT

Five different types of solar arrays have been tested in large vacuum chamber. Arc inception voltages, arc rates, and current collections are measured for samples with different coverglass materials and thickness, interconnect designs, and cell sizes. It is shown that the array with wrapthrough interconnects have the highest arc threshold and the lowest current collection. Coverglass design with overhang results in decrease of current collection and increase of arc threshold. Doubling coverglass thickness does not improve measured array parameters. Both arc inception voltage and current collection increase significantly with increasing a sample temperature to 80 C. Sustained discharges are initiated between adjacent cells with potential differences of 40 V for the sample with 300  $\mu\text{m}$  coverglass thickness and 60 V for the sample with 150  $\mu\text{m}$  coverglass thickness.

### INTRODUCTION

The main obstacle to the implementation of a high-voltage solar array in space is arcing on the conductor-dielectric junctions exposed to the surrounding plasma. One obvious solution to this problem would be the installation of fully encapsulated solar arrays which were not having exposed conductors at all. However, there are many technological difficulties that must be overcome before the employment of fully encapsulated arrays will turn into reality. An alternative solution to rise arc threshold by modifications of conventionally designed solar arrays looks more appealing, at least in the nearest future. A comprehensive study of arc inception mechanism [1-4] suggests that such

modifications can be done in the following directions: i) to insulate conductor-dielectric junction from a plasma environment (wrapthrough interconnects); ii) to change a coverglass geometry (overhang); iii) to increase a coverglass thickness; iiiii) to outgas areas of conductor-dielectric junctions. The operation of high-voltage array in LEO produces also the parasitic current power drain on the electrical system. Moreover, the current collected from space plasma by solar arrays determines the spacecraft floating potential that is very important for the design of spacecraft and its scientific apparatus. In order to verify the validity of suggested modifications and to measure current collection five different solar array samples have been tested in large vacuum chamber. Each sample (36 silicon based cells) consists of three strings containing 12 cells connected in series. Thus, arc rate and current collection can be measured on every string independently, or on a whole sample when strings are connected in parallel. The heater installed in the chamber provides the possibility to test samples under temperature as high as 80 C that simulates the LEO operational temperature. The experimental setup is described below.

### 1. EXPERIMENTAL SETUP

Low Earth Orbit (LEO) plasma environment was simulated in the large vacuum tank (1.8 m diameter and 3 m height). The vacuum equipment provided pressure as low as 0.5  $\mu\text{Torr}$ . One Kaufman source was installed to generate argon (or xenon) plasma with electron density  $n_e=(0.1-10)\cdot 10^5 \text{ cm}^{-3}$ , temperature  $T_e=0.6-1.2 \text{ eV}$ , and neutral gas pressure  $p=(0.7-7)\cdot 10^{-5} \text{ Torr}$  which could be kept steady during the experiment. To measure plasma parameters, two Langmuir probes with diameter 2 cm were employed. To determine an ion distribution function and to improve measurements of electron temperature one retarding potential analyzer (RPA) was mounted on the bottom of the tank. It was found that the ion (xenon) thermal flux in the experiment is about three times lower than ram ion flux in LEO,

---

\*Senior Scientist, Member AIAA

<sup>\*</sup>Physicist, Member AIAA

<sup>§</sup>Group Leader, Member AIAA

and the electron temperature is 5-10 times higher than in ionosphere. However, the number densities are simulated with a quite high accuracy, and one can believe that the results of high-voltage experiments in vacuum chambers are fairly adequate to the outcomes of processes in LEO plasma. To control plasma chemical composition (particularly, water vapor and oil partial pressures) a quadruple mass spectrometer was installed.

The sample (or set of samples) is vertically mounted in the middle of the chamber, and it is biased to a voltage power supply through a capacitor and a 10 k $\Omega$  resistor network back to ground. An additional power supply (Solar Array Simulator-SAS) is used to generate electrical field perpendicular to the dielectric side surface for investigating arc inception on semiconductor-dielectric junction and inception of sustained discharges between adjacent strings. Diagnostic equipment includes two current probes to measure discharge current and SAS current, and one voltage probe that allows us to register voltage pulse on the sample during the discharge (Fig.1). The most probable arcing sites are determined by employing a video camera and VCR. Most experiments were performed at room temperature (15C), but some tests had been done at the temperature +80 C simulating the exposure of solar array to full sun in LEO.

## **2. ARCING IN PLASMA**

Five types of tested solar arrays are shown in Table 1. Each string (12 cells in series) is tested separately to measure arc inception voltage and arc rate. Measurements reveal significant differences in these parameters even for strings belonging to one sample. There are two reasons explaining such observations: manufacturing process peculiarities and geometrical design of a sample. In fact, the middle string is separated from neighboring strings by narrow gaps (0.8 mm) covered with a thin RTV layer while two other strings have edges with underlying semiconductor and dielectric exposed to the plasma. Manufacturing peculiarities demonstrate themselves when one compares arc parameters for two outer strings and finds considerable differences. And arc sites are located mostly on interconnects for middle string while great part of arcs on outer strings has been observed on cell edges. To preserve the homogeneity of collected data one common experimental procedure is used for all measurements of arc inception voltages and arc rates: 1) string is initially biased to voltage well below an expected arcing threshold; 2) 15-30 minute time interval is allowed to

register (or to not register) an arc; 3) voltage is increased on 10-20 V; 4) arc rate is defined as an average over a respective time span. On the first stage of the test, two samples (#1 and #2 in Table 1) are mounted on the heater plate and installed in chamber. The results of measurements at the room temperature are shown in Fig.2. Unexpectedly, arc inception voltage is lower for the panel with higher coverglass thickness, and arc rates are close to each other. Strange trend of decreasing arc rate with increasing voltage is also observed for both strings. One possible explanation of this trend is that measurements are performed near respective arc thresholds. It will be demonstrated below that this trend alters to the normal when arc rate is high. Arc rates have been also determined at high temperature (Fig.3). Arc rates are widely scattered over a range of voltages 280-380 V, and using thick coverglass does not decrease an arc rate. In general, the temperature rise to 80 C results in significant increase of arc inception voltage (40-60 V). In particular, inner strings are not arcing below 300 V. It is worth noting that measurements shown above have been done at comparatively high water vapor partial pressures: 4  $\mu$ Torr at 15 C, and 15-30  $\mu$ Torr at 80 C. These values are much higher than one can anticipate in LEO conditions. Arc rate on the middle string of Sample #2 has been determined for two different water vapor pressures at high temperature while other plasma parameters are kept steady (Fig.4). Surprisingly, arc rate is found higher for lower partial pressure even though arc inception voltage does not change. Moreover, arc inception voltage at room temperature decreases from 280 V to 240 V for this string after one thermal circle. Finally, these two samples have been tested at room temperature after three thermal circles. Arc inception voltages are determined to be somewhat higher (40 V) comparatively to initial values for middle strings while other strings do not show any significant changes(Fig.5).

To test the possibility of outgassing of the whole sample by heating it to 80 C and pumping out an excess of water vapor the sample #2 has been undergone to five thermal circles. Arc rates are measured for all three strings connected in parallel at room temperature before the first circle and after the fifth circle. The results are shown in Fig.6. Background water vapor pressure has been decreased about three times (from 1.3  $\mu$ Torr to 0.4  $\mu$ Torr) but the influence of thermal circling on arc rate is rather weak. On the other hand, the degree of outgassing stays unclear because the measurements of water vapor partial pressures at

high temperature indicate high values ( $\sim 30 \mu\text{Torr}$ ) even for the last circle. The decrease of an arc rate during the process of continuing arcing (conditioning) has been measured by biasing the whole sample #2 to  $-400 \text{ V}$  and measuring average arc rate for every four minutes (Fig.7). Additional capacitance is increased to  $1\mu\text{F}$  to accelerate conditioning. After about 70 arcs, arc rate drops from  $3.25 \text{ arc/min}$  to the magnitude of  $1 \text{ arc/min}$  and stays practically steady for the next 30 arcs. To verify the influence of plasma density on arc rate this parameter has been increased by factor 1.5, and arc rate was measured for the next 100 arcs. Finally, arc rate has decreased to  $0.25 \text{ arc/min}$  after about 200 arcs. Thus, the influence of conditioning on previous measurements of arc rates for separate strings belonging to different samples is insignificant, particularly because of low capacitance ( $0.22 \mu\text{F}$ ) used in these tests. Arcing on the sample #3 (CMX UVR coverglass) does not show any measurable differences comparatively to arcing on previous samples. Arc inception voltage for the middle string is  $300 \text{ V}$ , and two other strings are arcing at lower voltages due to considerable percentage of arcs on the cell edges. On the contrary, the test results for the sample #5 ( $250 \mu\text{m}$  overhang) look much more prospective. Arc inception voltage is  $80\text{-}100 \text{ V}$  higher, and arc rate is lower for the middle string (Fig.8). Two other strings have also demonstrated the decrease of arc rate in spite of arcing on cell edges. The increase of arc inception voltage to  $480 \text{ V}$  for the hot sample is particularly important. It seems that the array with coverglass overhang and additional insulation of cell edges can operate at  $400 \text{ V}$  in LEO conditions. According to existing model of arc inception the most probable arc site on an array surface is a conductor-dielectric junction exposed to the plasma. Thus, if all interconnects are insulated from the surrounding plasma the probability of a discharge decreases significantly. One of the possible realizations of this idea is the array design with wrapthrough interconnects (sample #5). Such design cannot prevent arcing at very high potential because edge of semiconductor (silicon, germanium, or other) stays exposed to the plasma, and many tests (including ones described in this paper) have demonstrated intensive arcing on cell edges. However, considerable increase of arc inception voltage can be expected, particularly for the middle string. Test results confirm these expectations (Fig.9). The inception of arc is observed on the middle string at bias voltage  $440 \text{ V}$  that is  $60 \text{ V}$  higher than arc inception voltage for the string with coverglass overhang. Arc sites are located

between adjacent cells belonging as to middle string as to neighboring strings. Two other strings demonstrate much lower arc inception voltages due to arcing on edges. Unfortunately, experimental setup has not provided a possibility to heat this sample above room temperature but even the results obtained to date show that this kind of solar array can be used in LEO to generate power at voltage  $450 \text{ V}$  if array edges are electrically insulated. Short electrostatic discharges studied above are certainly undesirable events that must be prevented for reliable operation of the spacecraft. However, this kind of transients are not damaging solar array irreversibly. Sustained discharges initiated between adjacent cells with a few tens volt potential difference are much more dangerous [5,6] because they can destroy cells and underlying substrate that results in considerable loss of power. Samples #1, #2, and #4 have been tested against an inception of sustained arc between two strings. The circuitry diagram for the test is shown in Fig.1. Test starts with lower limits on SAS voltage and current. After the registration of 5-10 arcs these parameters are gradually changed and more arcs are generated until initial sign of sustained discharge is seen on the oscilloscope. This sign represents the SAS current pulse that continues much longer than original arc (Fig.10). The corresponding SAS current and voltage are considered as threshold parameters because even a small increase of them ( $10 \text{ V}$  and  $0.25 \text{ A}$ ) results in spectacular event shown in Fig. 11. In this case the sustained discharge has been quenched after 20 s by turning SAS off. Damaged part of the sample is shown in Fig.12. Threshold parameters depend on solar array design: they are  $40 \text{ V}$  and  $1 \text{ A}$  for sample #1,  $60 \text{ V}$  and  $2 \text{ A}$  for sample #2, and  $80\text{V}$  and  $1.6 \text{ A}$  for sample #4.

### **3.SCALING OF ARC PARAMETERS**

Even short transients are detrimental for spacecraft, and the degree of damage increases with the increase of arc current amplitude and pulse width. These two parameters depend on the amount of electrical charge leaking into surrounding plasma during the discharge time. There are currently two theoretical models that allow estimating lost electrical charge and its dependence on the array capacitance. First model [7] is based on the suggestion that the discharge generates an expanding plasma sheath neutralizing positive charge on top of coverglass. If plasma expands with a constant speed the discharge time is proportional to the array linear

dimensions, or, in another terms, to the square root of an array capacitance. This dependence has been proved in many experiments [8,9]. However, the distance that plasma can expand on is limited to about 1 m in simulated LEO conditions [10]. Thus, according to the first model the upper limit for the effective capacitance is the capacitance of the part of solar array with area approximately 1 m<sup>2</sup>. The second model also envisages that both arc current amplitude and pulse width are proportional to the square root of a capacitance but this prediction is based on the dynamics of ionization-recombination processes in the discharge plasma [11]. If the second model is correct the effective capacitance is only two-three times less than the capacitance of a whole solar array. A simple experiment has been performed to verify the validity of the second model. Two solar array samples (sample #2) are mounted on aluminum panel with grounded aluminum plate installed between samples. The height of the plate is 7.5 cm bigger than the distance between aluminum panel and top of the sample. Such arrangement prevents the expansion of plasma sheath from one sample to another. The additional capacitor of 1000 pF is used in this particular experiment. The capacitance of one cell can be calculated as

$$C_1 = \frac{\epsilon_0 \epsilon_1 S_1}{d_1} \left( 1 + \frac{\epsilon_1 d_2}{\epsilon_2 d_1} \right)^{-1} \quad (1)$$

Dielectric constants for coverglass material and adhesive are poorly known. However, a quite reliable estimate can be obtained by assuming  $\epsilon_1=6.7$  and  $\epsilon_2=3$ :  $C_1=600$  pF/cell. Moreover, the scaling does not practically depend on exact numbers for largest capacitances. Ten measurements of arc current pulse widths for each configuration have been done by biasing one string, three strings, and six strings in parallel. The results are shown in Fig.13. The scaling is confirmed with a very high accuracy, which means that adequate ground simulations of arcing on spacecraft surfaces have to be performed with a very large additional capacitance (for instance, about 1000 pF for ISS).

#### 4. CURRENT COLLECTION

One solar cell provides current of 1 A in order of magnitude while collected current is scaled in hundred microamps. Thus, the role of collected current in a parasitic power drain is certainly

negligible. However, the floating potential of the spacecraft strongly depends on the current collected by the solar array [12]. There are three main factors that influence on a magnitude of collected current: i) solar array design; ii) solar array temperature; iii) parameters of surrounding plasma. Obviously, the design with coverglass overhang and with wrapthrough interconnects offers arrays with considerably decreased collected currents. Electron number density and electron temperature also influence on current collection. Ground tests that simulate an electron component of LEO plasma quite reasonably provide reliable data for current collection by cells with positive potentials with respect to surrounding plasma. Test data containing measurements of collected current for negatively biased cells are applicable to the analysis of spacecraft floating potential not better than in order of magnitude because the characteristics of ion component are different in ground tests and in LEO.

The dependence of electron current collection on bias voltage is shown in Fig.14. It is seen that the increase of electron number density results in the almost proportional increase in current collection. But the dominant factor in the current collection is an array temperature. The magnitude of collected current grows more than three times when array temperature reaches 79 C. This observation must be taken into account for the computations of spacecraft floating potentials. Ion currents are measured by biasing separate strings up to 100 V negative, and these currents do not exceed 1  $\mu$ A for all situations studied even though the same effect of significant increase due to heating is also found. Measurements of collected currents for the sample with coverglass overhang have demonstrated the decrease in magnitude close to the factor 2 comparatively to sample with a standard design (Fig.15). Cell with wrapthrough interconnects collects not much less current than cell with coverglass overhang but it generates three times higher power. It seems that tests in simulated plasma environment are suitable for creation a data base for further computations of the spacecraft floating potentials in LEO.

#### 5. CONTAMINATION OF PLASMA ENVIRONMENT

When spacecraft is coming out of eclipse, solar array temperature is rising due to exposure to Sun radiation. Operational temperature of an array in LEO conditions is approximately 80-100 C. It is believed that the adsorbed contaminants from the

array surface are evaporating at a high rate due to heating. On another hand, when solar array sample is installed in a vacuum chamber its surface is contaminated not only by “natural” species (adsorbed water, atmospheric gases, and products of a technological process) but also other contaminants. The most abundant of these contaminants is vacuum pump oil. To measure chemical composition of background vacuum and to determine plasma contamination due to heating, the quadruple mass-spectrometer is installed in large chamber. Two solar array samples consisting of 36 cells (4x6 cm) each are mounted on an aluminum sheet with electrical heater placed on the back (Fig.16). This heater provides enough power to radiately heat sample from 15 C to 80 C for about 40 minutes (Fig.17). It is seen that the increase in water vapor

partial pressure is considerably higher than the plain isochoric increase  $\frac{\Delta p}{p_0} = \frac{\Delta T}{T_0}$ , and this

observation confirms the presence of water adsorbed on solar array surface. In spite of using cooled traps (-40 C) for diffusion pumps, a significant concentration of oil cannot be prevented. Even keeping samples in vacuum for two days does not result in decrease of oil partial pressure below 1  $\mu$ Torr (Fig.18). The lower limit was found for water vapor also: 1  $\mu$ Torr is the lowest pressure achieved after one week continuous operation. Such partial pressure corresponds to a comparatively high number density ( $10^{10}$  cm<sup>-3</sup>). Thermal flux of water molecules toward the solar array surfaces can reach more than  $10^{15}$  cm<sup>-2</sup>s<sup>-1</sup>, and this is enough to adsorb a few molecular layers on porous surface in a minute time span. Thus, it is impossible to avoid the contamination of solar array surface by water and oil vapors with current experimental equipment. The use of cryogenic pump instead of diffusion pump seems particularly important for testing large solar array samples when the effect of conditioning is slowed down by a large area of conductor-dielectric junctions.

## **CONCLUSIONS**

Comprehensive tests of five different types of solar array samples in simulated LEO plasma environment have demonstrated that the highest arc threshold (440 V) can be achieved for an array with wrapthrough interconnects if edges of strings are not exposed to the plasma. This design is also effective in decreasing of an array current collection. The design with exposed interconnects but with coverglass overhang also provides significant improvement comparatively to the

conventional design. Particularly, arcing on the sample cannot be initiated at potentials below 300 V even under room temperature, and arc threshold increases to 420 V under temperature 72 C. The increase of coverglass thickness itself appears to be useless in this respect. The potential difference between adjacent cells must be lower than 40 V in order to avoid an initiation of a sustained discharge.

## **Acknowledgements**

Authors are greatly thankful to Frank Lam for help with the experiment.

## **References**

1. Cho, M., and Hastings, D.E. “Computer Particle Simulation on High-Voltage Solar Array Arcing Onset”, *Journal of Spacecraft and Rockets*, Vol.30, No.2, 1993, pp.189- 205.
2. Soldi, J.D., Hastings, D.E., Hardy, D., Guidice, D., and Ray, K. “Flight Data Analysis for the Photovoltaic Array Space Power Plus Diagnostics Experiment”, *Journal of Spacecraft and Rockets*, Vol.34, No.1, 1997, pp.92-103.
3. Ferguson, D.C., Snyder, D.B., Vayner, B.V., and Galofaro, J.T. “Array Arcing in Orbit- From LEO to GEO”, *AIAA Paper 99-0218*, Jan. 1999.
4. Upschulte, B.L., Marinelli, W.J., Carleton, K.L., Weyl, G., Aifer, E., and Hastings, D.E. “Arcing on Negatively Biased Solar Cells in a Plasma Environment”, *Journal of Spacecraft and Rockets*, Vol.31, No.3, 1994, pp.493-501.
5. Hoeber, C.F., Robertson, E.A., Katz, I., Davis, V.A., and Snyder, D.B. “Solar Array Augmented Electrostatic Discharge in GEO”, *AIAA Paper 98-1401*, Jan. 1998.
6. Snyder, D.B., Ferguson, D.C., Vayner, B.V., and Galofaro, J.T. “New Spacecraft- Charging Solar Array Failure Mechanism” 6<sup>th</sup> Spacecraft Charging Technology Conference, Nov. 2-6, 1998, Air Force Res. Lab., Hanscom AFB, MA, USA, pp.297- 301
7. Balmain, K. G., and Dubois, G. R. “Surface Discharges on Teflon, Mylar and Kapton”, *IEEE Transactions on Nuclear Science*, Vol. 26, No.12, 1979, pp.5146-5151.
8. Snyder, D.B. “Characteristics of Arc Currents on a Solar Cell Array in a Plasma”, *IEEE Transactions on Nuclear Science*, Vol.31, No.4, 1984, pp.1584-1587.
9. Vayner, B., Galofaro, J., and Ferguson, D. “Arc Inception Mechanism on a Solar Array Immersed in a Low-Density Plasma”, *Proceedings of 7<sup>th</sup> Spacecraft Charging Technology Conference*, Noordwijk, The Netherlands, April 23-27, 2001,

pp.469-474.

10. Cho, M., Ramasamy, R., Hikita, M., Tanaka, K., and Sasaki, S. "Plasma Response to Arcing in Ionospheric Plasma Environment: Laboratory Experiments", Journal of Spacecraft and Rockets, Vol.39, No.3, 2002, pp.392-408

11. Vayner, B., Galofaro, J., Ferguson, D., and Degroot, W. "Electrostatic Discharge Inception

on a High-Voltage Solar Array", AIAA Paper 2002-0631, Jan.2002.

12. Ferguson, D.C., and Hillard, G.B. "In-Space Measurements of Electron Current Collection by Space Station Solar Arrays", AIAA Paper 95-0486, Jan. 1995.

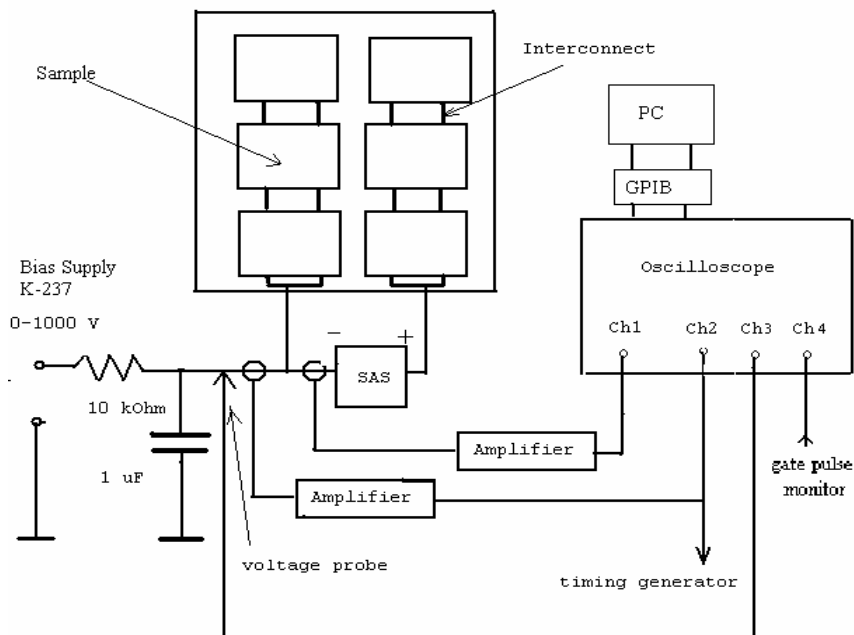
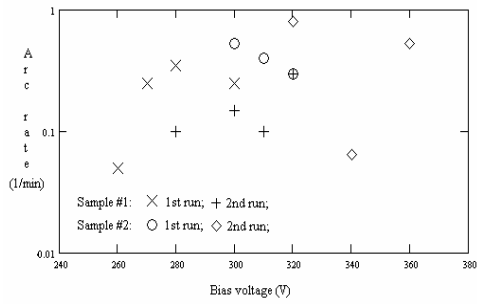


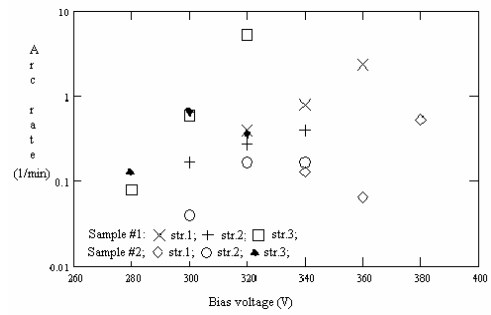
Fig.1. Circuitry diagram for arc inception study.

Table.1 Five types of solar array samples tested in the large chamber.

Sample No	Coverglass Thickness (μm)	Material	Overhang (μm)	Cell size (cm)	Interconnect
1	300	UVR	0	4x6	exposed
2	150	UVR	0	4x6	exposed
3	150	CMX UVR	0	4x6	exposed
4	150	UVR	250	4x6	exposed
5	150	UVR	0	8x8	wrapthrough



**Fig.2.** Arc rates are shown for middle strings of two samples at 15 C.



**Fig.3.** Arc rates at the temperature 80C

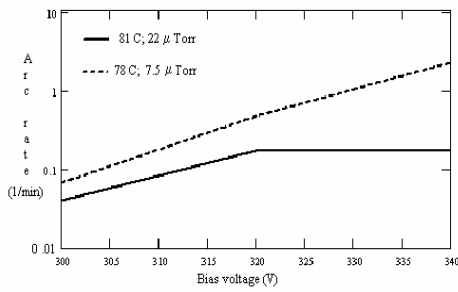


**Fig.4.** Arc rates are shown for middle strings under different water vapor partial pressures.

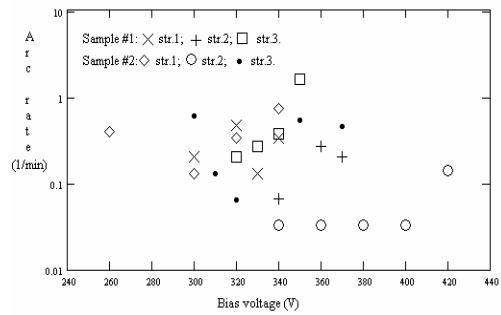


**Fig.5.** Arc rates are shown for all strings after three thermal circles

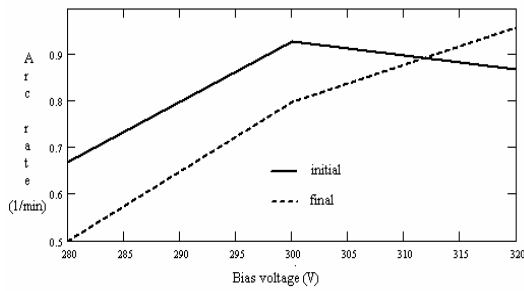


**Fig.6.** Change in arc rate for sample #2 after five thermal circles.

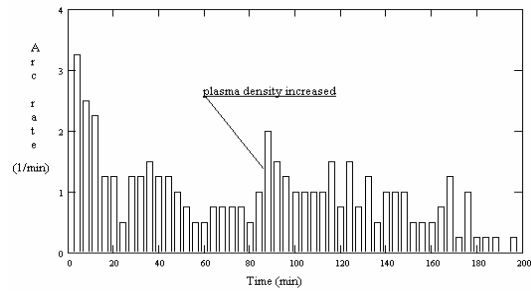


**Fig.7.** Decreasing of arc rate in the process of arcing (conditioning) for sample #2.

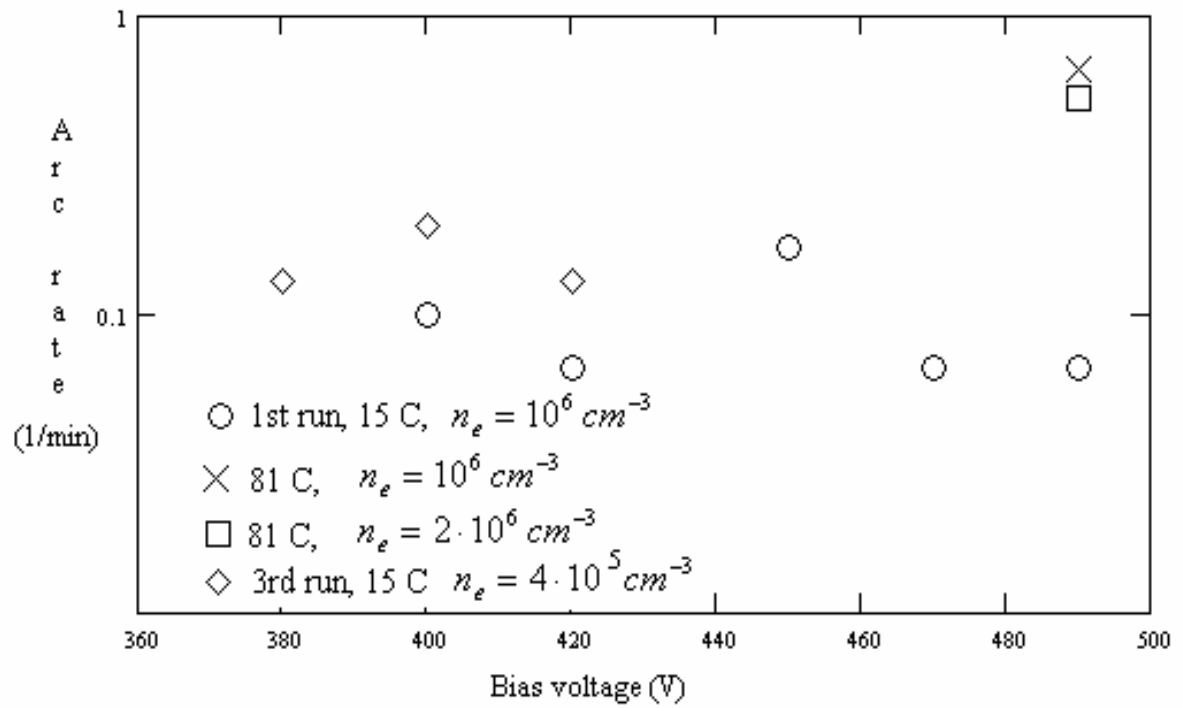


**Fig.8.** Arc rates are shown under different conditions for the middle string of sample #4

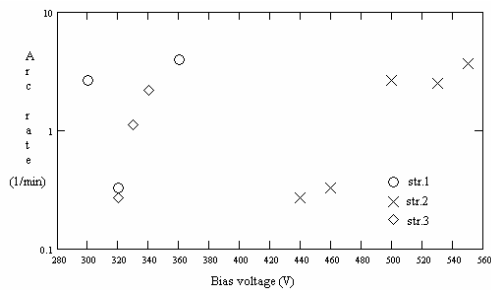


**Fig.9.** Arc rates for sample #5.

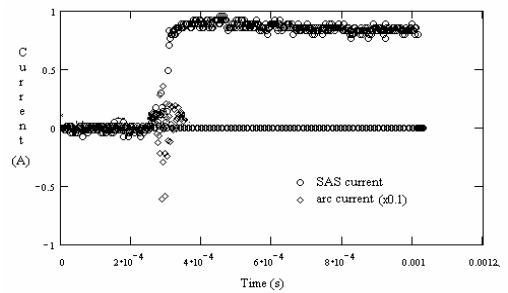


**Fig.10.** Both arc current and SAS current pulse forms are shown for a sustained arc.



**Fig.11.** One frame of a 20 s long video record of a sustained arc

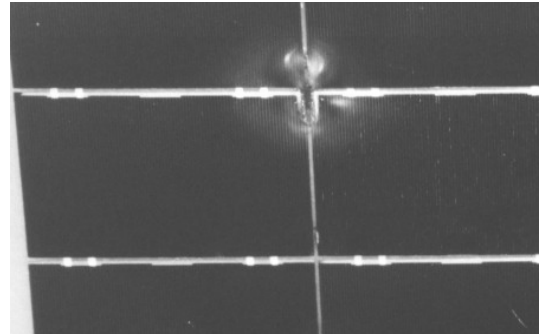


**Fig.12.** Damage induced by sustained arc.

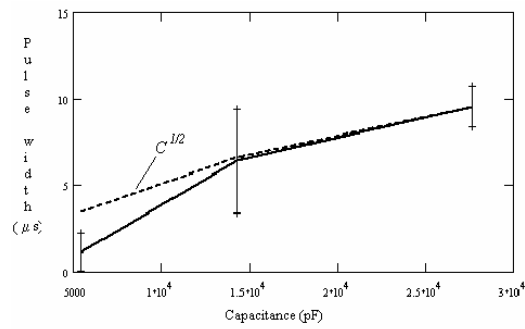


**Fig.13.** Pulse width scaling measured by biasing to -340 V one, three, and six strings of sample #2. Error bars ( $\pm 1\sigma$ ) are calculated from ten measurements for each point.

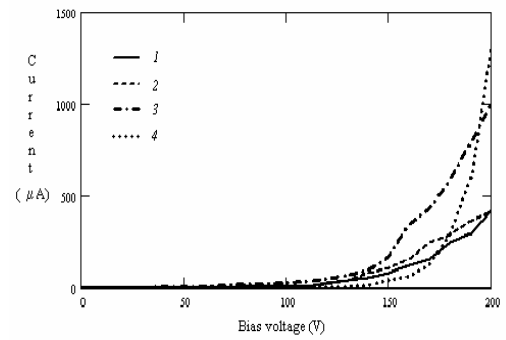


**Fig.14.** Current collection: 1-sample #2, str.2,  $n_e=2*10^5 \text{ cm}^{-3}$ , 15 C; 2-sample #1, str.1,  $n_e=7*10^5 \text{ cm}^{-3}$ , 15 C; 3-sample #1, str.2,  $n_e=2*10^6 \text{ cm}^{-3}$ , 15 C; 4-sample #2, str.1,  $n_e=5*10^5 \text{ cm}^{-3}$ , 79 C.

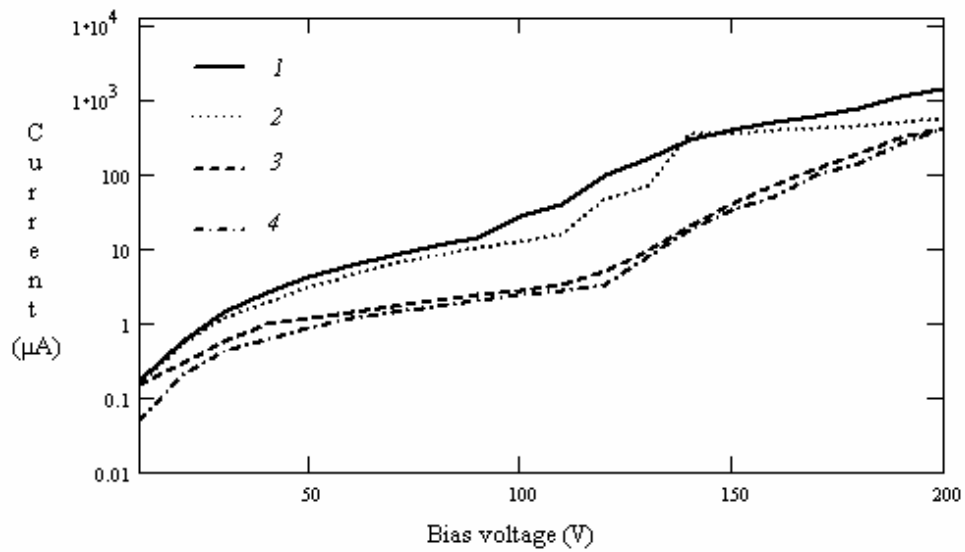


**Fig.15.** Current collections are shown at 15 C for samples with coverglass overhang and wrapthrough interconnect designs: 1-sample #3, str.2,  $n_e=1*10^6 \text{ cm}^{-3}$ ; 2- sample #4, str.2,  $n_e=1*10^6 \text{ cm}^{-3}$ ; 3 and 4-sample #5, str.1 and 2 respectively,  $n_e=3.5*10^5 \text{ cm}^{-3}$ .

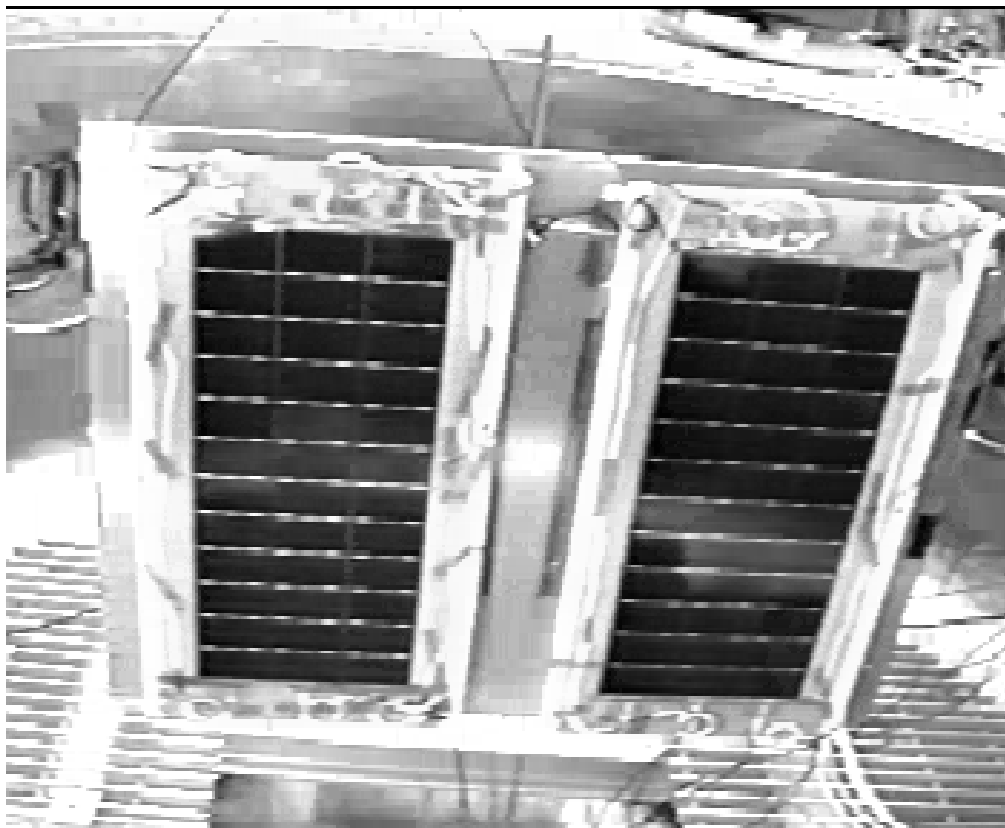


**Fig.16.** Two solar array samples mounted on aluminum radiator.

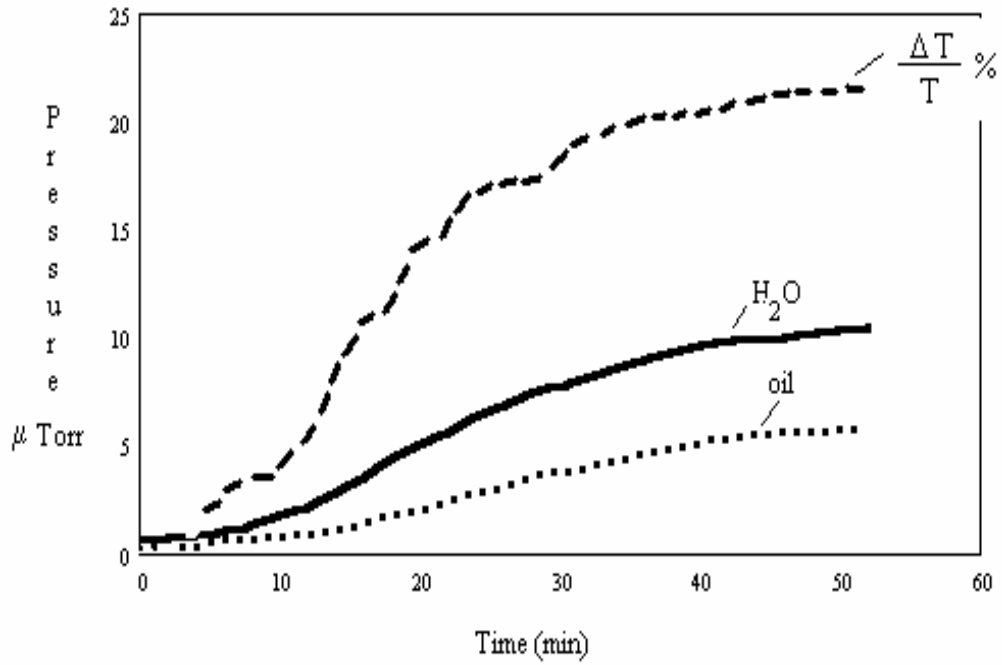


**Fig.17. Increase of water vapor and oil partial pressures is significantly higher than the expected isochoric increase.**

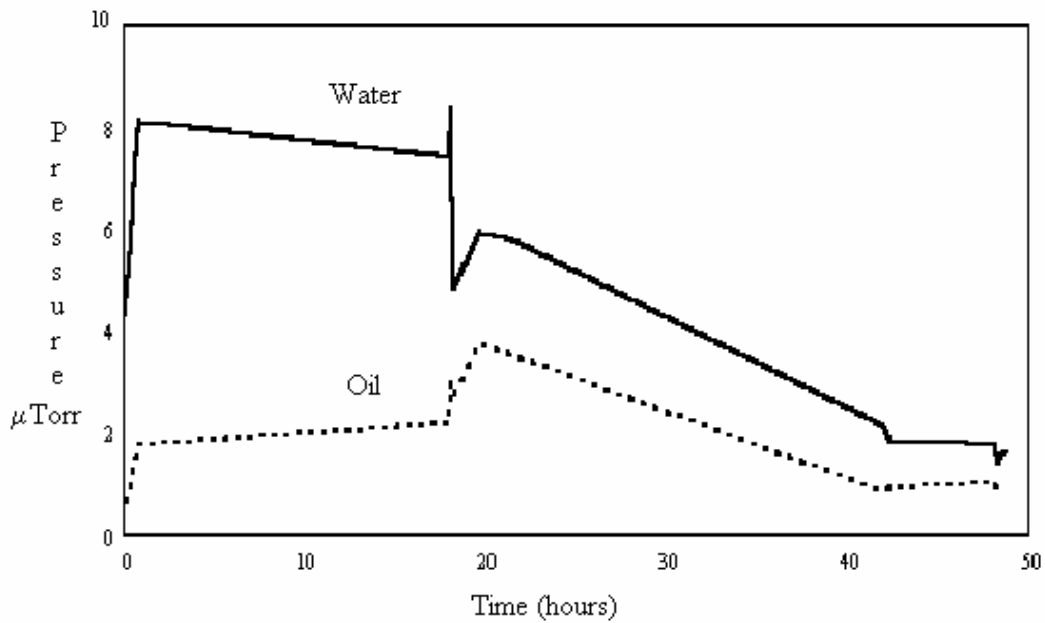


**Fig.18. Heating-cooling circles resulted in significant cleaning of array surface.**